COMPOSITE REINFORCEMENT FORMING SIMULATION: A MULTISCALE APPROACH

N. Hamila – A. Khan – S. Gatouillat – E. De Luycker –
E. Vidal-Sallé – T. Mabrouki – P. Boisse
[1]Université de Lyon, LaMCoS, INSA-Lyon
Philippe.Boisse@insa-lyon.fr

SUMMARY

The finite elements presented in this paper for textile fabric forming are composed of woven unit cells. The mechanical behaviour of these is analyzed by 3D computations at the mesoscale regarding biaxial tensions, in plane shear and bending properties. These elements are efficient because they are close to the physics of the woven cell while avoiding the very large number of unknowns in the discrete approach. Forming simulations on single ply, multi-ply and 3D interlock will be presented and show the efficiency of the approach. In particular the importance of the in-plane shear and bending behaviour will be emphasized.

Keywords: Composite Forming; forming/draping simulations, textile composite, meso-macro

INTRODUCTION

To accurately perform mechanical analyses of composite materials, it is necessary to know the direction and the density of the fibres at any point on the part. These directions are mainly dependent on the forming of the composite. Woven textile reinforcements can reach very large in-plane shear strain during manufacturing when the final shape is double curved. A numerical tool that simulates this forming process determines not only the conditions of the feasibility of a process without defect but also the directions of the reinforcements after shaping. In addition to the mechanical behaviour of the final solid composite, the angles between warp and weft yarns influence the permeability of the reinforcement and thus the filling of the resin in the case of a liquid moulding process [1].

To simulate draping of textile composite reinforcement, several packages are commercially available based on “kinematical models” [2]. This method is very fast but does not account for the mechanical behaviour of the woven reinforcement for possible sliding of the fabric in relation to the tools and for load boundary conditions. These points are very important in the case of forming with punch and die (such as in the preforming of the R.T.M. process). A complete physical simulation of a composite forming process needs a model of the mechanical behaviour woven reinforcement and usually a numerical method, for instance, the finite element method. The mechanical behaviour of fabrics is complex due to the intricate interactions of the yarns. It is a multi-scale problem. The macroscopic behaviour is very dependent on the interactions of yarns at the meso-scale (scale of the woven unit cell) and at the micro-scale (level of the fibres constituting yarns). Despite the many works in the field, there is no widely

accepted model that accurately describes all the main aspects of a fabric mechanical behaviour. A first family of models considers the fabric as an anisotropic continuum [3-6], the mechanical behaviour of which has to take into account the influence of the underlying meso-structure. While these models can be easily integrated in F.E. standard shell or membrane elements, the identification of homogenized material parameters is difficult, especially because these parameters change when the fabric is subjected to the large strains due to forming. At the opposite, some authors present discrete models of fabrics based on modelling of the woven yarns usually described by simplified elements such as beams and springs [7-8]. A major difficulty lies in the very large number of components at mesoscale and the very large number of contacts with friction between them.

This paper is based on the semi-discrete approach [9]. As in the discrete approach, the components at the mesoscale are considered (yarns, or woven cells). But in the case of the semi-discrete approach, they are part of finite elements and their strains are given by the node displacements. The corresponding strain energy is computed from mechanical behaviour obtained from experimental tests that are specific to the textile composite reinforcements. By considering the behaviour of the woven unit cell, the semi-discrete approach allows only the significant mechanical properties of the element at mesoscale to be taken into account. This leads to numerically efficient elements. The difficulty of determining the equivalent continuous mechanical behaviour for the fibrous material at large strains is avoided on one hand and on the other hand the number of unknowns is greatly reduced in comparison to the discrete approaches.

The bending stiffness of textile reinforcement is very small due to its fibrous nature Nevertheless this second order rigidity can be important in some cases especially when some wrinkles appear. This paper presents a shell element composed of woven cells and rotational-free i.e. with only displacements nodal variables [10]. A set of example including draping and forming simulations are presented in order to show the efficiency of the proposed shell element and to highlight the influence and importance of the tensile, in plane shear and bending rigidities.

THE SEMI-DISCRETE APPROACH FOR TEXTILE COMPOSITE REINFORCEMENT

The textile material results from the assembly of continuous fibres with a very small diameter. It exhibits a very specific mechanical behaviour since relative motions are possible between the yarns and the fibres. In LCM processes (Liquid Composite Moulding), the textile reinforcement pre-forming stage takes advantage of these possible motions. The forming is made on dry reinforcement (i.e. without resin) since it is performed before the injection stage.

In the present work the approach is called semi-discrete. The textile composite reinforcement is seen as a set of a discrete number of unit woven cells submitted to membrane (i.e. biaxial tension and in-plane shear) and bending (Figure 1).

In any virtual displacement field $\underline{\eta}$ such as $\underline{\eta} = 0$ on the boundary with prescribed loads, the virtual work theorem relates the internal, exterior and acceleration virtual works:

$$W_{ext}(\underline{\eta}) - W_{int}(\underline{\eta}) = W_{acc}(\underline{\eta}) \quad \text{with} \quad W_{int}(\underline{\eta}) = W_{int}^{t}(\underline{\eta}) + W_{int}^{s}(\underline{\eta}) + W_{int}^{b}(\underline{\eta}) \qquad (1)$$

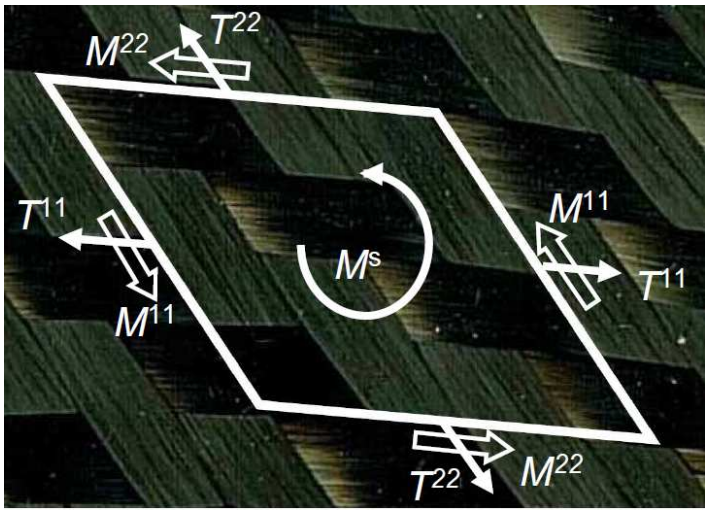

Figure 1. Unit woven cell submitted to tension, in-plane shear and bending

$W_{int}^{t}(\underline{\eta})$, $W_{int}^{s}(\underline{\eta})$, $W_{int}^{b}(\underline{\eta})$ are the internal virtual works of biaxial tension, in-plane shear and bending respectively with :

$$W_{int}^{t}(\underline{\eta}) = \sum_{p=1}^{ncell} {}^{p}\varepsilon_{11}(\underline{\eta})\ {}^{p}T^{11}\ {}^{p}L_1 + {}^{p}\varepsilon_{22}(\underline{\eta})\ {}^{p}T^{22}\ {}^{p}L_2 \qquad (2)$$

$$W_{int}^{s}(\underline{\eta}) = \sum_{p=1}^{ncell} {}^{p}\gamma(\underline{\eta})\ {}^{p}M^{s} \qquad (3)$$

$$W_{int}^{b}(\underline{\eta}) = \sum_{p=1}^{ncell} {}^{p}\chi_{11}(\underline{\eta})\ {}^{p}M^{11}\ {}^{p}L_1 + {}^{p}\chi_{22}(\underline{\eta})\ {}^{p}M^{22}\ {}^{p}L_2 \qquad (4)$$

where ncell is the number of woven cell. L_1 and L_2 are the length of unit woven cell in warp and weft directions. $\varepsilon_{11}(\underline{\eta})$ and $\varepsilon_{22}(\underline{\eta})$ are the virtual axial strain in the warp and weft directions. $\gamma(\underline{\eta})$ is the virtual angle between warp and weft directions. $\chi_{11}(\underline{\eta})$ and $\chi_{22}(\underline{\eta})$ are the virtual curvatures of warp and weft directions. $\varepsilon_{11}(\underline{\eta})$, $\varepsilon_{22}(\underline{\eta})$, $\gamma(\underline{\eta})$, $\chi_{11}(\underline{\eta})$ and $\chi_{22}(\underline{\eta})$ are function of the gradient of the virtual displacement field. T^{11} and T^{22} are the tensions on the unit woven cell in warp and weft directions. M^{11} and M^{22} are the bending moments on the woven cell respectively in warp and weft directions. M^{s} is the in-plane shear moment. The mechanical behaviour of the textile reinforcement defines a relation between the loads $T^{\alpha\alpha}$, M^{s}, $M^{\alpha\alpha}$ and the strain field. Experimental tests specific to textile composite reinforcements are used to obtain these mechanical properties. The biaxial tensile test gives the tensions T^{11} and T^{22} in function of the axial strain ε_{11} and ε_{22} [11], the picture frame or the bias extension test gives the shear moment M^{s} in function of the angle change γ between warp and weft yarns [12] and the bending test give the bending moments $M^{11}$and M^{22} in function respectively of χ_{11} and

χ_{22} [13]. An alternative consists in virtual tests i.e. in 3D simulations of the deformation of a unit woven cell submitted to elementary loadings such as biaxial tensions or in plane shear [14] (Figure 2).

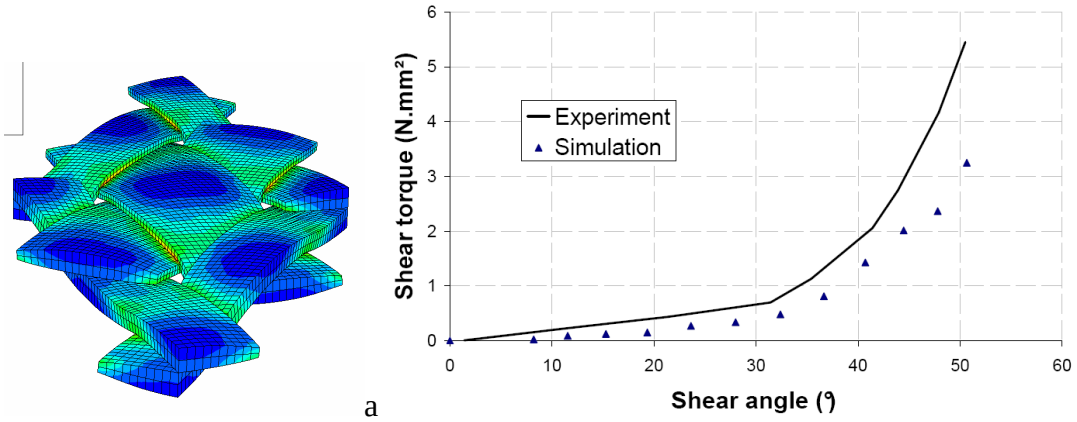

a b

Figure 2. Shear of woven fabric: (a) Mesoscopic F.E. analysis: deformed unit cell (b) Experimental and numerical shear curve

The tensions T^{11} and T^{22} simultaneously depend on the warp and weft strains because of the weaving i.e., they are in the form $T^{11}(\varepsilon_{11}, \varepsilon_{22})$, $T^{22}(\varepsilon_{11}, \varepsilon_{22})$. The in-plane shear moment is assumed to depend only on the shear angle i.e. $M^s(\gamma)$. Bending moments are supposed to be in the form $M^{11}(\chi_{11})$ and $M^{22}(\chi_{22})$. The above forms of the loads $T^{\alpha\alpha}$, M^s, $M^{\alpha\alpha}$ in function of the strains in the unit woven cell are used because they account for the main phenomena, because other data are usually not available and also in order to keep the approach simple enough. Some studies have shown that these simplifications can be questionable in some cases [15]. Nevertheless it is possible to extend the approach to the cases where each load $T^{\alpha\alpha}$, M^s, $M^{\alpha\alpha}$ depends on more strain components.

Triangular element made of woven cells

The three node triangle shown figure 3 is composed of ncelle woven cells. The natural material coordinates ξ^1, ξ^2 are defined along the sides of the element. These coordinates have the following values at the nodes of the triangle : $M_1(0,0)$, $M_2(1,0)$, $M_3(0,1)$. The displacement $\underline{u}$ and the position $\underline{x}$ of a point P within the element are interpolated from the values at node:

$$\underline{u}(P) = \sum_{i=1}^{3} N_i \underline{u}(M_i) \qquad \underline{x}(P) = \sum_{i=1}^{3} N_i \underline{x}(M_i) \tag{5}$$

With $N_1 = 1 - \xi^1 - \xi^2$ $\quad N_2 = \xi^1$ $\quad N_3 = \xi^3$ (6)

The material coordinates r^1, r^2 are defined along the warp and weft directions (figure 3). r^1 is equal to zero on M_1M_3 and is equal to 1 in M_2. r^2 is equal to zero on M_1M_2 and equal to 1 in M_3.

The material vectors $\underline{k}_1$, $\underline{k}_2$ are defined from r^1, r^2:

$$\underline{k}_1 = \frac{\partial \underline{x}}{\partial r^1} \qquad \underline{k}_2 = \frac{\partial \underline{x}}{\partial r^2} \qquad \text{and consequently} \qquad \underline{k}_1 = \underline{AM}_2 \qquad \underline{k}_2 = \underline{BM}_3 \tag{7}$$

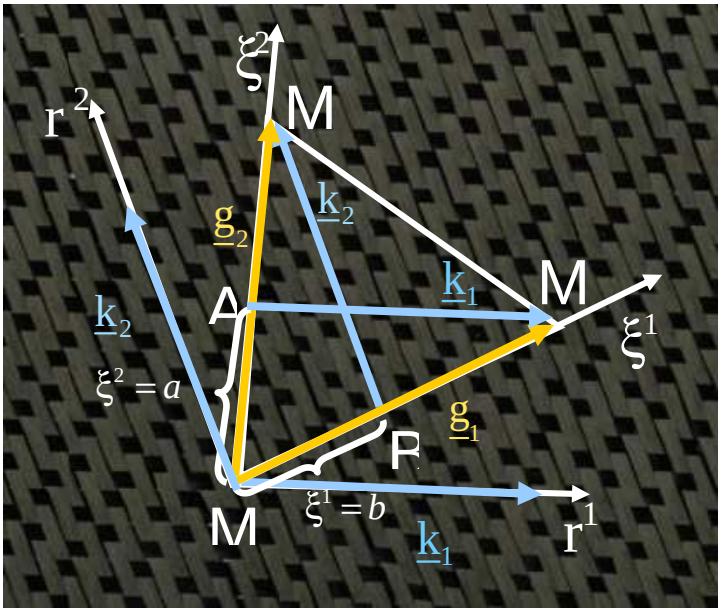

Figure 3. Three node finite element made of woven cells

Nodal membrane internal loads

The virtual displacement gradient can be expressed in the warp and weft frame (figure 3):

$$\underline{\underline{\nabla^s}}(\underline{\eta}) = \frac{1}{2}\left(\frac{\partial \underline{\eta}}{\partial r^\alpha}\cdot \underline{k}_\beta + \frac{\partial \underline{\eta}}{\partial r^\beta}\cdot \underline{k}_\alpha\right)\underline{k}^\alpha \otimes \underline{k}^\beta \qquad (8)$$

Consequently the elementary tensile virtual work can be written :

$$W_{int}^{te}(\underline{\eta}) = \boldsymbol{\eta}_n^{eT}\mathbf{F}_{int}^{te} = \left(\sum_{p=1}^{ncelle} {}^pB_{1ij}\,{}^pT^{11}\,{}^pL_1\frac{{}^pL_1}{\|\underline{k}_1\|^2} + {}^pB_{2ij}\,{}^pT^{22}\frac{{}^pL_2}{\|\underline{k}_2\|^2}\right)\eta_{ij} \qquad (9)$$

with

$B_{1i1} = (a\text{-}1)k_{1i}$ $\quad B_{1i2} = k_{1i}$ $\quad B_{1i3} = -ak_{1i}$

$B_{2i1} = (b\text{-}1)k_{2i}$ $\quad B_{2i2} = -bk_{2i}$ $\quad B_{2i3} = k_{2i}$ $\qquad (10)$

The elementary nodal tensile interior loads are determined. Because of the linear interpolation, the strain interpolation terms $B_{\alpha ij}$ are very simple and constant in the element. The strains and consequently the tensions are constant in the element, consequently:

$$\left(F_{int}^{te}\right)_{ij} = ncelle\left(B_{1ij}T^{11}\frac{L_1}{\|\underline{k}_1\|^2} + B_{2ij}T^{22}\frac{L_2}{\|\underline{k}_2\|^2}\right) \qquad (11)$$

The angle variation between warp and weft directions in the virtual field virtual $\gamma(\underline{\eta})$ is given by the gradient of the virtual displacement:

$$\gamma(\underline{\eta}) = \left(\underline{\underline{\nabla}}\underline{\eta}\cdot\underline{f}_1\right)\cdot\underline{f}^2 + \left(\underline{\underline{\nabla}}\underline{\eta}\cdot\underline{f}_2\right)\cdot\underline{f}^1 \qquad (12)$$

with

$$\underline{f}_1 = \frac{\underline{k}_1}{\|\underline{k}_1\|}, \underline{f}_2 = \frac{\underline{k}_2}{\|\underline{k}_2\|}, \underline{f}^1 = \frac{\underline{k}^1}{\|\underline{k}^1\|}, \underline{f}^2 = \frac{\underline{k}^2}{\|\underline{k}^2\|} \qquad (13)$$

The expression of the components of the virtual displacement gradient (8) gives the interpolation of the virtual angle variation $\gamma(\underline{\eta})$:

$$\gamma(\underline{\eta}) = \left(B_{1ij} \frac{\underline{k}^1}{\|\underline{k}_1\|} \cdot \frac{\underline{k}^2}{\|\underline{k}^2\|} + B_{3ij} \frac{\|\underline{k}^2\|}{\|\underline{k}_1\|} + B_{4ij} \frac{\|\underline{k}^1\|}{\|\underline{k}_2\|} + B_{2ij} \frac{\underline{k}^2}{\|\underline{k}_2\|} \cdot \frac{\underline{k}^1}{\|\underline{k}^1\|} \right) \eta_{ij} = B_{\gamma ij} \eta_{ij} \qquad (14)$$

with:

$B_{3i1} = (b-1)k_{1i}$ $\quad B_{3i2} = -bk_{1i}$ $\quad B_{3i3} = k_{1i}$

$B_{4i1} = (a-1)k_{2i}$ $\quad B_{4i2} = k_{2i}$ $\quad B_{4i3} = -ak_{2i}$ $\qquad (15)$

$B_{\gamma i1}$, is constant in the three node finite element, therefore

$$\left(F_{int}^{se}\right)_{ij} = \text{ncelle } B_{\gamma ij} M^s(\gamma) \qquad (16)$$

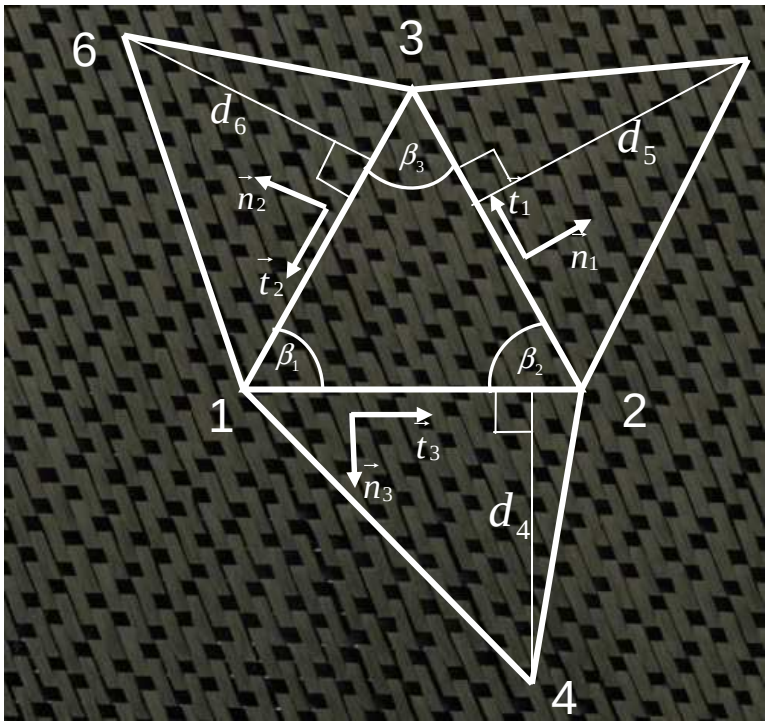

Figure 4. Triangular element and its 3 neighbours

In order to avoid to add supplementary degrees of freedom and consequently for numerical efficiency, the bending stiffness is taken into account within an approach without rotational degree of freedom [10]. In theses approaches the curvatures of the element are computed from the positions and displacements of the neighbouring nodes elements (Figure 4). The details of the formulation can be found in [16]. It gives the interpolations of the curvatures in warp and weft directions are now defined:

$$\chi_{\alpha\alpha}(\underline{\eta}) = Bb_{\alpha km} \eta_{km} \qquad (17)$$

m= 1 to 6 (index of the node), k = 1 to 3 (index of direction of the displacement).
The nodal bending interior load components are:

$$\left(F_{int}^{be}\right)_{km} = n_{celle}\left(Bb_{1km}M^{11}\frac{L_1}{\left\|\underline{k}_1\right\|^2} + Bb_{2km}M^{22}\frac{L_2}{\left\|\underline{k}_2\right\|^2}\right) \quad (18)$$

FORMING SIMULATIONS

Draping on a cylinder of revolution

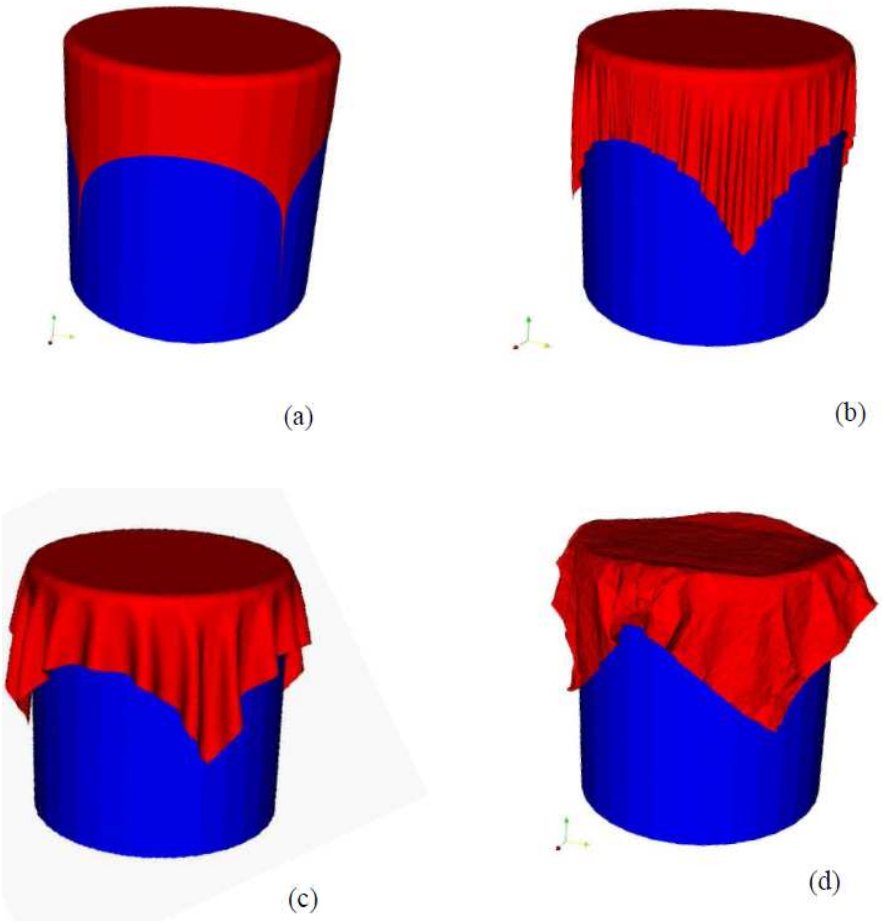

Figure 5. Draping on a circular cylinder

An initially flat square fabric is draped on a cylinder (figure 5). Four different mechanical behaviour models are considered: tensile stiffness only (Figure 5a), tensile and in-plane shear stiffness (Figure 5b), tensile, in-plane shear and bending stiffness (Figure 5c). The deformed shape obtained when only tensile stiffness is taken into account involves very large shear angle in the corners of the fabric but no wrinkle. Wrinkles appear when in-plane shear stiffness is taken into account and shear angles are limited (Figure 5b). The size of the wrinkles is larger and more realistic when the bending stiffness of the fabric is taken into account (Figure 5c). In Figure 5d, an isotropic behaviour is used for the sheet. For instance it could be a paper sheet. The draping is not possible. The required large shear angles in the corners are not allowed by this behaviour for which the in-plane shear behaviour is related to the tensile one. That shows the very important role of the in-plane shear behaviour in draping/forming of

membrane. A textile can be shaped on a double curved surface because there are possible large rotations between warp and weft yarns and in-plane shear stiffness is weak. In the case of an isotropic membrane that is not possible. On the other hand the shear stiffness that increases when the shear angle becomes large leads to wrinkles. If this shear stiffness is neglected there will be no wrinkle in any case.

Very unbalanced fabric forming

The hemispherical forming of a 2x2 nylon twill is analysed (figure 6). This fabric is used in automotive industry. It presents a very unbalanced tensile behaviour in warp and weft direction. The warp rigidity is 50 N/yarn and the weft rigidity is 0.2 N/yarn. The shear behaviour of this fabric has been analysed by the picture frame test. Experimental tests of the hemispheric sheet forming have been achieved in the composites laboratory of the University of Nottingham. The blank holder is a 6 kg ring submitted to its own weight. The final shape obtained after forming is very asymmetrical. There is a large axial strain in the weft direction (horizontal) and large displacements with very small axial strain in the warp direction (vertical). This final shape is well obtained by the simulation. The ratio of the lengths after deformation l_{weft}/l_{warp} is equal at the top of the hemisphere to 1.8 in experiments and in simulation as well. There are many wrinkles, especially along the vertical axis. They are fairly well obtained by the simulation.

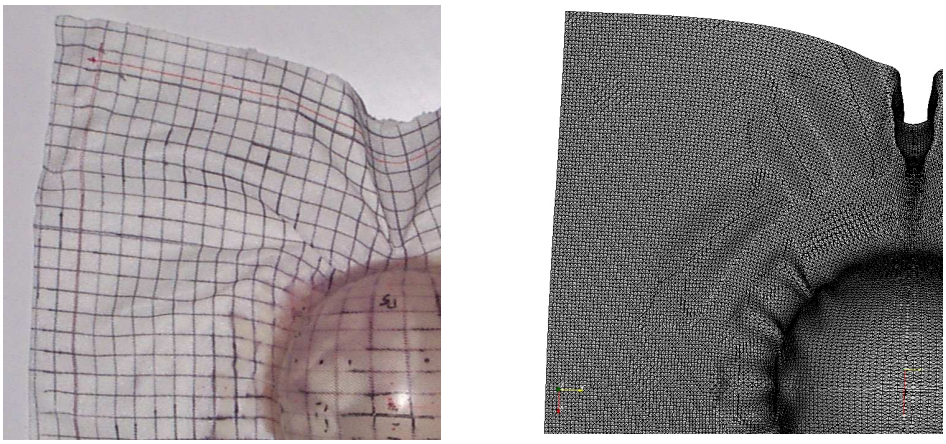

Figure 6. Hemispherical forming of an unbalanced fabric.
Simulation (right) and experiment (left)

CONCLUSIONS

The semi-discrete finite element described in this paper is an alternative to continuous and discrete approach for textile composite reinforcement forming. The virtual work of internal loads is composed of a tensile part, an in plane shear part and a bending part. The tensions, shear and bending moments included in the nodal internal loads are directly those that are measured by the specific experimental tests that are used for characterising textile composite reinforcements.

The proposed finite element is numerically efficient because only the significant quantities are computed in these internal loads and also because the element is rotational free. It has been shown that the in-plane shear stiffness is of main important for wrinkle appearance and that bending stiffness determine the shape of those wrinkles.

ACKNOWLEDGEMENTS

The support from the French research ministry and of the Rhône-Alpes region (MACODEV) is gratefully acknowledged

REFERENCES

1. Bickerton S., Simacek P. Guglielmi S.E., Advani S.G., Investigation of draping and its effects on the mold filling process during manufacturing of a compound curved composite part. Composite Part A, 1997, 28, 801-816.

2. Van Der Ween F., Algorithms for draping fabrics on doubly curved surfaces. Int. J. of Num. Meth. in Eng. 31, 1414-1426 (1991)

3. Spencer A.J.M., Theory of fabric-reinforced viscous fluid. Composites Part A 31, 1311-1321 (2000)

4. Peng X., Cao J., A continuum mechanics-based non-orthogonal constitutive model for woven composite fabrics. Composites Part A, 36, 859–874 (2005)

5. Ten Thije RHW, Akkerman R, Huetink J., Large deformation simulation of anisotropic material using an updated Lagrangian finite element method. Computer methods in applied mechanics and engineering 2007; 196(33–34): 3141–3150.

6. Badel P, Gauthier S, Vidal-Salle E, Boisse P., Rate constitutive equations for computational analyses of textile composite reinforcement mechanical behaviour during forming. Composites Part A (2008), On line, doi : 10.1016/j.compositesa.2008.04.015

7. Durville D., Modélisation par éléments finis des propriétés mécaniques de structures textiles : de la fibre au tissu. European Journal of Computational Mechanics, 11(2-3-4), 463-477 (2002)

8. Pickett A. K., Review of finite element methods applied to manufacturing and failure prediction in composite structures. Applied Composite Material 9, 43-58 (2002).

9. Boisse P, Zouari B, Gasser A., A mesoscopic approach for the simulation of woven fibre composite forming. Composites science and technology 2005; 65 (3-4): 429-436.

10. Onate E, Zarate F., Rotation-free triangular plate and shell elements. International Journal For numerical Methods In Engineering 2000; 47:557-603

11. Buet-Gautier K, Boisse P., Experimental analysis and modeling of biaxial mechanical behavior of woven composite reinforcements. Experimental Mechanics 2001; 41 (3): 260-269.

12. Cao J, Akkerman R, Boisse P, Chen J et al., Characterization of Mechanical Behavior of Woven Fabrics: Experimental Methods and Benchmark Results. Composites Part A 2008; 39: 1037–1053

13. de Bilbao E, Soulat D, Hivet G, Launay J, Gasser A., Bending Test of Composite Reinforcements, Int J Mater Form DOI 10.1007/s12289-008-0265-z Springer/ESAFORM 2008

14. P. Badel, E. Vidal-Salle, E. Maire, P. Boisse, Simulation and tomography analyzis of textile composite reinforcement deformation at the mesoscopic scale, Composites Science and Technology 68 (2008) 2433–2440

15. Lomov SV, Verpoest I., Model of shear of woven fabric and parametric description of shear resistance of glass woven reinforcements. Composites Science and Technology 2006; 66: 919–933.

16. Hamila, P. Boisse, F. Sabourin, M. Brunet, A semi-discrete shell finite element for textile composite reinforcement forming simulation, Int. J. Numerical Methods in Engineering, Accepted 2009, In press

Previous Paper *Back to Programme* *Back to Topic* *Next Paper*